Gold Nanoparticles Synthesized Using Various Reducing Agents and the Effect of Aging for DNA Sensing

Yuzhe Ding, Po-Jung Jimmy Huang, Mohamad Zandieh, Jinghan Wang and Juewen Liu*

Department of Chemistry, Waterloo Institute for Nanotechnology, Waterloo, ON, N2L 3G1, Canada

Email: liujw@uwaterloo.ca

Abstract

Citrate-capped gold nanoparticles (AuNPs) are one of the most commonly used reagents in colloidal science and biosensor technology. In this work, we first compared AuNPs prepared using four different reducing agents including citrate, glucose, ascorbate and 4-(2-hydroxyethyl)-1-piperazineethanesulfonic acid (HEPES). At the same absorbance at the surface plasmon peak of 520 nm to 530 nm, citrate-AuNPs and glucose-AuNPs adsorbed more DNA and achieved higher affinity to the adsorbed DNA. In addition, citrate-AuNPs had better sensitivity than glucose-AuNPs for label-free DNA detection. Then, using citrate-AuNPs, the effect of aging was studied by incubation of the AuNPs at 22°C (room temperature) and at 4°C for up to 6 months. During aging, the colloidal stability and DNA adsorption efficiency gradually decreased. In addition, the DNA sensing sensitivity also dropped around 4-fold after 6 months. Heating at boiling temperature of the aged citrate-AuNPs could not rejuvenate the sensing performance. This study shows that while citrate-AuNPs are initially better than the other three AuNPs in their colloid properties and sensing properties, this edge in performance might gradually decrease due to constantly changing surface properties caused from the aging effect.

Introduction

The excellent optical and surface properties of gold nanoparticles (AuNPs) enabled it as a highly attractive material for developing biosensors.[1-8] For various applications, the most common method to synthesize AuNPs in aqueous solutions is by reducing hydrogen tetrachloroaurate ($HAuCl_4$) with citrate.[9, 10] By simply varying the concentration of citrate, the size of the synthesized AuNPs can be tuned from around 12 nm to over 100 nm.[11] Extensive studies have been performed to understand the adsorption of citrate on AuNPs and its displacement by other molecules.[12-14] It is generally accepted that while citrate is weakly adsorbed and easily displaced, clusters of citrate might interact laterally leading to highly stable adsorption.[13, 15]

Aside from citrate, many other reducing agents can also be used to synthesize AuNPs. For example, sodium borohydride produces much smaller AuNPs of around 3-5 nm.[16] However, on top of its low extinction coefficient, its small size makes it inconvenient for centrifugation. As a result, sodium borohydride is not a popular reducing agent for preparing AuNPs for colorimetric sensing. Other common reducing agents include glucose, ascorbate and even buffer molecules such as HEPES.[17] In particular, HEPES was used for preparing gold nanostars.[18] When different reducing agents are used, the resulting AuNPs have different sizes and shapes and most importantly, different surface molecules. These surface ligands can in turn affect the property of AuNPs.[19]

An important application of AuNPs is to adsorb DNA so that it can be used for designing biosensors,[2, 4, 20, 21] assembling nanomaterials,[6, 22, 23] and for drug delivery.[3, 24, 25] By modifying the surface ligands, these properties can change significantly in terms of the kinetics and capacity for DNA adsorption.[19] DNA adsorption can then be used to probe the surface chemistry of AuNPs.[19, 26] So far, the majority of DNA adsorption and biosensor studies were performed using citrate-capped AuNPs. Thus, interesting comparisons can be made between AuNPs prepared using other reducing agents. For example, the adsorption of glucose on AuNPs might be weaker than citrate since glucose has only hydroxyl groups. In the current study, we aimed to prepare a series of AuNPs containing surface ligands with different adsorption affinities.

The other aspect to explore is the aging-dependent performance of AuNPs. It was recently reported that the citrate adsorption on AuNPs changes slowly over time.[14] We wondered whether the colloidal properties and DNA-based sensing performance would differ between the freshly

prepared and the aged AuNPs. In this work, we prepared four types of AuNPs by various reducing agents and compared their DNA adsorption and biosensing properties side-by-side. In addition, citrate-capped AuNPs were also monitored for 6 months to observe the aging effect on biosensing.

Materials and Methods

Chemicals

All of the DNA samples were purchased from Integrated DNA Technologies (Coralville, IA, USA), and their sequences are listed in Table 1. $HAuCl_4$ and sodium L-ascorbate were purchased from Sigma-Aldrich (St. Louis, MO). Sodium chloride (NaCl), glucose, sodium citrate ($Na_3C_6H_5O_7$), disodium hydrogen phosphate (Na_2HPO_4), sodium dihydrogen phosphate (NaH_2PO_4), and 4-(2-hydroxyethyl) piperazine-1-ethanesul-fonate (HEPES) were from Mandel Scientific (Guelph, ON, Canada). Milli-Q water was used to prepare all of the buffers and solutions.

Table 1. The DNA sequences used in this work.

DNA names	Sequences (5′ to 3′)
24-mer	ACG CAT CTG TGA AGA GAA CCT GGG
c24-mer	CCC AGG TTC TCT TCA CAG ATG CGT
FAM-DNA	AAA AAA AAA CCC AGG TTC TCT-FAM

Instrumentation

The transmission electron microscopy (TEM) images were taken using a Phillips CM10 100 kV microscope. The ζ-potential values were measured by a dynamic light scattering (DLS) instrument (Zetasizer Nano 90, Malvern). The fluorescence measurements were performed using a microplate reader (Tecan Spark). The Ultraviolet-visible (UV-vis) absorption spectra were collected using an Agilent 8453A spectrometer.

Synthesis of AuNPs

The citrate-capped AuNPs were prepared by the Turkevich method. In a typical synthesis, 100 mL 1 mM $HAuCl_4$ was heated to reflux under magnetic stirring, and then 10 mL 38.8 mM sodium citrate was quickly added.[27, 28] After refluxing for another 20 min, the heating was turned off and

the stirring was continued until cooled naturally to room temperature. The HEPES-reduced AuNPs were synthesized by mixing 1 mL $HAuCl_4$ (10 mM) with 9 mL HEPES (50 mM, pH 7.4) with vigorous stirring at room temperature.[29] The glucose-reduced AuNPs were prepared by mixing 200 μL $HAuCl_4$ (0.05 M) and 50 mL glucose (0.03 M) under stirring for 30 min, and then 3 mL NaOH (0.25 M) was added dropwise.[30] The ascorbate-reduced AuNPs were prepared by stirring 50 mL $HAuCl_4$ (0.5 mM) in a flask at room temperature followed by adding 0.5 mL sodium-L-ascorbate (0.1 M).[31]

Colloidal stability of AuNPs

To test the colloidal stability of the four kinds of AuNPs, different concentrations of NaCl up to 150 mM were added. After incubation for 1 min, the UV-vis absorption spectra of the samples were collected. For determining the degree of aggregation, the extinction ratio at two wavelengths (A_{620}/A_{525}) was used.

DNA adsorption

For the salt-assisted DNA adsorption method, 100 nM FAM-DNA, 45 mM phosphate buffer (pH 7.5), 50 mM NaCl and each of the four kinds of AuNPs (diluted to a similar UV absorbance) were either incubated for 10 min or overnight at room temperature. To achieve the same absorbance, the ascorbate-AuNPs were diluted 3.3-fold, the citrate and HEPES AuNPs were diluted 5-fold, and the glucose-AuNPs were diluted 1.25-fold. After centrifugation of the samples for 15 min at 15000 rpm, 5 μL of the supernatants were mixed with 95 μL 5 mM pH 7.5 phosphate buffer in a 96-well microplate for fluorescence measurement (excitation 485 nm, emission 535 nm, F_1). In addition, the pellets were washed with 5 mM phosphate buffer once and then dissolved using 30 mM KCN to fully release the adsorbed FAM-DNA from the AuNPs. Similarly, 5 μL of the KCN treated solution was mixed with 95 μL 5 mM pH 7.5 phosphate buffer for fluorescence measurement (F_2). The fraction of DNA adsorption was determined by $F_2/(F_1+F_2)$. For the acid-assisted DNA adsorption method, 100 nM FAM-labeled DNA, 40 mM citrate buffer (pH 3) and the four kinds of AuNPs were incubated for 10 min at room temperature. The other steps followed the same procedure as the salt-assisted method. For the citrate-AuNPs aging experiment, the same batch of 2 nM AuNPs aged at different lengths of time, 100 nM FAM-labeled DNA, 45 mM phosphate buffer (pH 7.5) and 50 mM NaCl were incubated for 10 min at room temperature, and the other steps were the same as the salt-assisted method.

DNA desorption experiment

FAM-labeled DNA (50 nM), citrate buffer (pH 3, 40 mM) and the four kind of AuNPs (diluted to a similar UV absorbance) were incubated for 20 min at room temperature. 5 μL of the solution was mixed with 95 μL phosphate buffer (50 mM, pH 7.5) in a 96-well microplate for kinetic fluorescence measurement (excitation 485 nm, emission 535 nm). After 7 min of monitoring, 1 mM KCN was added. When the fluorescence became stable, 10 mM KCN was then added into the samples to fully dissolve the AuNPs. To test the aged AuNPs, 2 nM AuNPs, 100 nM FAM-labeled DNA, 45 mM phosphate buffer (pH 7.5) and 50 mM NaCl were incubated for 20 min at room temperature. Then, 5 μL of the solution was mixed with 95 μL phosphate buffer (5 mM, pH 7.5) in a 96-well microplate for kinetic fluorescence measurement.

DNA sensing tests

First, the 24-mer DNA probe and its cDNA were annealed at different ratios with a total DNA strand concentration of 1 μM in 100 mM NaCl. For the glucose-AuNPs, the DNA samples and 75 μL glucose-AuNPs were mixed followed by adding 47.2 mM phosphate buffer (pH 7.5) and 56.6 mM NaCl. After incubation for 10 min at room temperature, the UV-vis spectra of the samples were collected. For determine the degree of aggregation, the extinction ratio of at two wavelengths (A_{620}/A_{525}) was used. To test the effects on the citrate-reduced AuNPs, different concentrations of dsDNA, 6 nM citrate-AuNPs, 47.2 mM phosphate buffer (pH 7.5) and 56.6 mM NaCl were incubated for 10 min at room temperature. The other steps were the same as the glucose-AuNPs experiment.

Results and Discussion

Synthesis and characterization of AuNPs

We synthesized four types of AuNPs using citrate,[27] glucose,[30] ascorbate,[31] and HEPES[29] as reducing agents to react with $HAuCl_4$, respectively (Figure 1A). A photograph of these AuNPs is shown in Figure 1B, which illustrates that all the solutions were red. However, different shades of red are shown, which may be caused by the different initial $HAuCl_4$ concentrations and the final particle sizes. The color of the HEPES-reduced AuNPs was the deepest, whereas the color of the

glucose-reduced AuNPs was the lightest. The TEM images of the four kinds of AuNPs are showed in Figure 1C-F. The citrate-reduced AuNPs were spheres with a uniform diameter of 13 nm. For the HEPES-reduced AuNPs, the particle size had a broader distribution ranging from 6.5 nm to 43 nm. A broad size distribution is indicative of non-synchronized nucleation and growth, which could be related to the relatively weak reducing activity of HEPES. The change of color of the HEPES sample took the longest time of around 8 min. For the glucose-reduced AuNPs, their particle size was relatively uniform (~14 nm spheres with a few triangles). Finally, the ascorbate-reduced AuNPs were larger forming relatively uniform spheres of ~41 nm in diameter.

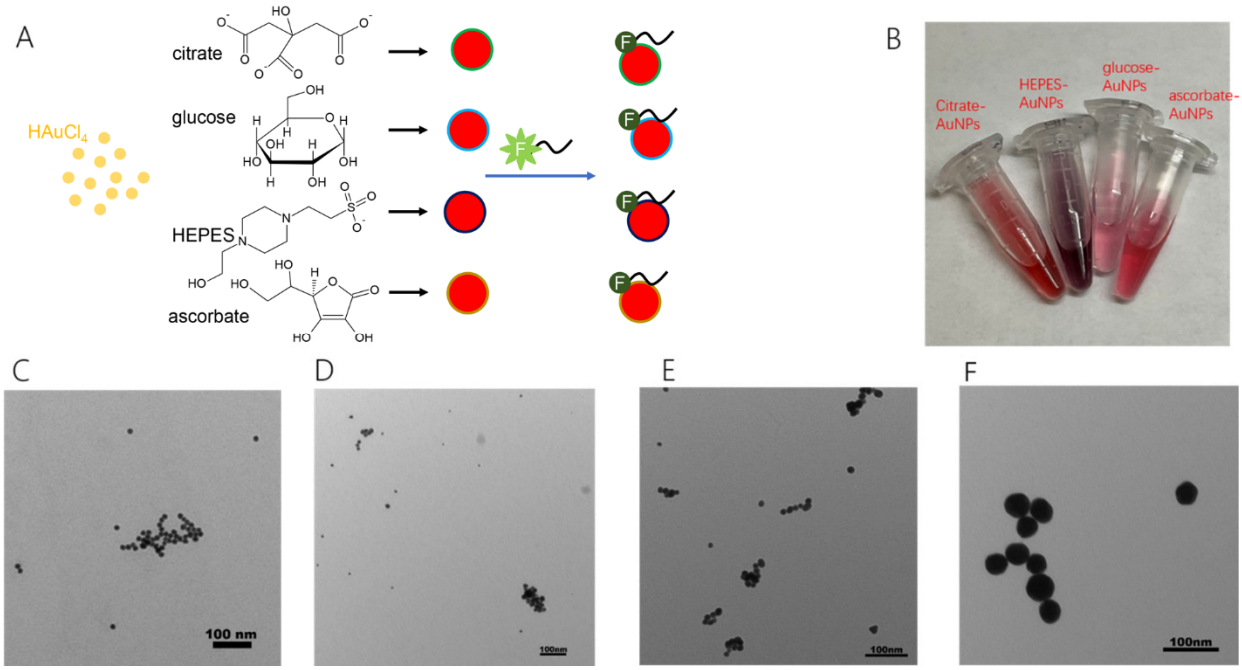

Figure 1: (A) Schematic of the synthesis of the four kinds of AuNPs and the adsorption of a FAM-labeled DNA resulting in quenched fluorescence. (B) A photograph of the four kinds of as-synthesized AuNPs. TEM micrographs of the AuNPs reduced by (C) citrate, (D) HEPES, (E) glucose, and (F) ascorbate. All the scale bars are 100 nm.

The AuNPs were then characterized using UV-vis spectroscopy (Figure 2A). We used the absorption peak height of the glucose-AuNPs as a reference and the other three AuNPs were diluted to match it. They all had a strong surface plasmon peak (520 nm for citrate-AuNPs, 526 nm for ascorbate and glucose-AuNPs, and 530 nm for HEPES-AuNPs). We then measured the ζ-

potential of the AuNPs (Figure 2B), all of which had a negative surface charge. The negative charges ensured charge stabilization for maintaining colloidal stability for all the AuNPs.

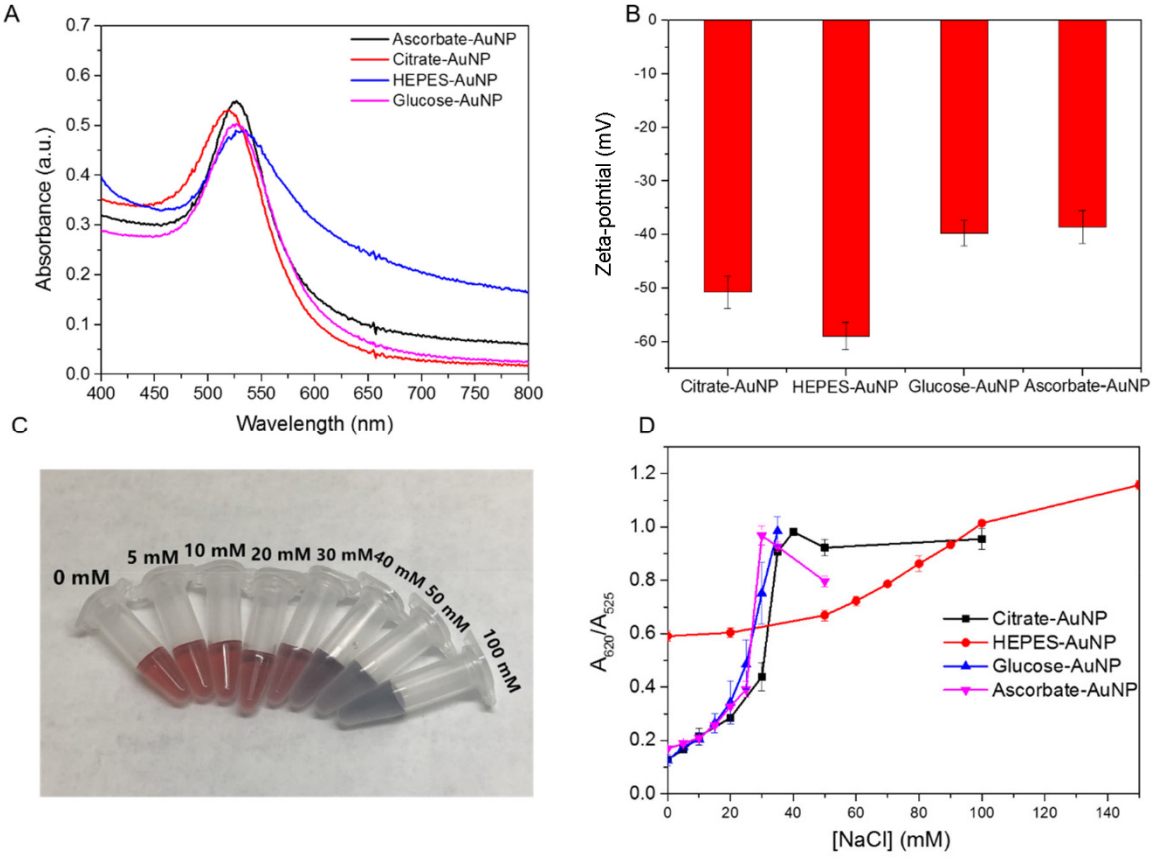

Figure 2. (A) UV-vis spectra, and (B) ζ-potential of the four types of AuNPs that were diluted to a similar absorbance around 0.5 at their plasmon peak. (C) A photograph showing the citrate-AuNPs incubated with different concentrations of NaCl. (D) The colloidal stability of the four types of AuNPs as a function of NaCl concentration evaluated using the absorbance ratio at 620 nm over 525 nm.

Colloidal stability of AuNPs

We first evaluated the colloidal stability of the AuNPs by challenging them with different concentrations of NaCl. NaCl would decrease the electrostatic repulsion between AuNPs and allow them to approach each other and aggregate. Such aggregation is accompanied with a color change due to the coupling of their surface plasmon. Figure 2C shows a photograph of citrate-AuNPs

mixed with increasing concentrations of NaCl, where the color gradually changed from red to purple to blue. This color change was then quantitatively measured by using UV-vis spectrometry. We chose the absorbance ratio at 620 nm over 525 nm to quantify the color change. For disperse AuNPs, this ratio was low, while upon aggregation, this ratio would increase. For the citrate-AuNPs (Figure 2D, black trace), the middle point of the transition was 32 mM NaCl. For the AuNPs that were reduced by glucose and ascorbate, their stabilities were slightly lower with middle points of 25 mM and 27 mM, respectively. Since the HEPES-AuNPs were larger in size, the initial ratio was much higher compared to the rest three. Nevertheless, a NaCl-dependent color change was still observed with a middle point of 80 mM NaCl. Thus, the ranking of the colloidal stability of these AuNPs followed HEPES > citrate > ascorbate ≅ glucose. This ranking, however, does not necessarily reflect the adsorption affinity ranking of these ligands. For example, glucose is a non-charged molecule and it is understandable that it has a lower stabilization effect. Citrate, on the other hand, has two or three negative charges (depending on the pH), and thus it can exert better charge stabilization. This stability information is useful for the subsequent DNA sensing studies.

DNA adsorption by AuNPs

We then studied the DNA adsorption properties of these four AuNPs based on fluorescence quenching. We respectively incubated a carboxyfluorescein (FAM) labeled DNA oligonucleotide with the four types of AuNPs for either 10 min or overnight, and 50 mM NaCl was added to promote DNA adsorption.[32] We adjusted all the AuNPs to have the same UV-vis peak height for colorimetric sensing, although their particle concentration or total surface area are likely different. Under this condition, the DNA:AuNP ratio was 50:1 for the citrate-capped AuNPs, and at this ratio, the DNA was not fully adsorbed (Figure S1). We measured DNA adsorption by quantifying the fluorescence intensity in the supernatants after centrifugation (Figure S2A, black bars). The citrate-AuNPs and glucose-AuNPs showed a similar capacity of DNA adsorption, and they both adsorbed more DNA than the HEPES-AuNPs and ascorbate-AuNPs.

To confirm DNA adsorption, we also collected the precipitates containing AuNP/DNA conjugates and then added 10 mM KCN to dissolve the AuNPs. In these samples, the reduced glucose-AuNPs and reduced citrate-AuNPs also had the highest fluorescence intensities (Figure

S2A, red bars), consistent with the data from the supernatants. Overall, for 10 min incubation, the adsorbed DNA was similar between the glucose-AuNPs and citrate-AuNPs (Figure 3A, black bars).

We also measured the DNA adsorption capacity after overnight incubation (Figure 3A, red bars, Figure S2B). For the ascorbate-AuNPs and HEPES-AuNPs, the adsorption efficiency did not change much compared to 10 min of incubation. Thus, for them, the system quickly reached an equilibrium and DNA could not be adsorbed more by simply increasing the incubation time. For the citrate-AuNP and glucose-AuNP, the amount of DNA adsorbed either remained the same or even decreased after overnight incubation compared to 10 min incubation (Figure 3A, red bars, Figure S2B). We reasoned that the decreased adsorption could be due to a gradual change of DNA conformation on AuNPs. Initially, a DNA might only adsorb on AuNPs via one or a few bases, and each AuNP could accommodate more DNA strands. Over time, some DNA strands might have more bases adsorbed, competing with the neighboring strands and desorbing some weakly adsorbed DNA strands. It is interesting to note that the citrate-AuNPs had more DNA adsorbed than the glucose-AuNPs after overnight incubation. It suggests that the DNA might initially adsorbed more easily on the glucose-AuNPs, which allowed for more conformational changes during the subsequent incubation. This result also suggests that glucose had a lower affinity to AuNPs compared to citrate. While the initial adsorption by the citrate-AuNPs and glucose-AuNPs was similarly high, we could only conclude that the adsorption affinity of citrate and glucose to AuNPs were both low. With the overnight data, we can better compare each type of AuNP to conclude stronger adsorption of citrate than glucose by AuNPs.

Since citrate appeared to allow for more rapid, efficient and stable DNA adsorption, to further evaluate the influence of reducing agents for DNA adsorption, we added various reducing reagents into the citrate-AuNPs. Then, with a DNA:AuNP ratio of 50:1, we measured the supernatant fluorescence intensity to quantify DNA adsorption (Figure 3B). HEPES inhibited DNA absorption, which was consistent with our previous results.[19] Adding glucose and ascorbate did not affect DNA absorption. This was an interesting result. We observed little DNA adsorption on the ascorbate-AuNPs. Yet, ascorbate did not inhibit the DNA adsorption to citrate-AuNPs.

Aside from the salt-assisted adsorption, we also tried the pH-assisted DNA adsorption method, which allows for more rapid and efficient results.[33 34] Except for replacing 50 mM NaCl with 40 mM pH 3 citrate buffer, the other conditions remained the same. The fraction of DNA

adsorption was higher for the pH-assisted method compared to the salt-assisted adsorption (Figure 3A, blue bars, Figure S2D). It appeared that the pH-assisted method was less sensitive to the initial surface ligand on AuNPs. Nevertheless, the ascorbate-AuNPs only adsorbed ~40% of the DNA, much lower than the other three types of AuNPs. The final oxidation products of ascorbate include threonate and oxalate, and based on their structures (number of carboxylic acid groups),[35] they are unlikely to be adsorbed more strongly than citrate to inhibit DNA adsorption. The ascorbate-AuNPs had the largest size and they may have a smaller total surface area compared to the other AuNPs of the same absorbance. Based on the initial $HAuCl_4$ concentration, size, and dilution factors at the same absorbance value, the surface area of the citrate-AuNPs was 4.2-fold higher compared to that of the ascorbate-AuNPs. We then used the as-prepared ascorbate-AuNPs without dilution (previously diluted 3.3-fold), and nearly 100% DNA adsorption was achieved (Figure S2E). Therefore, ascorbate-AuNPs can also effectively adsorb DNA.

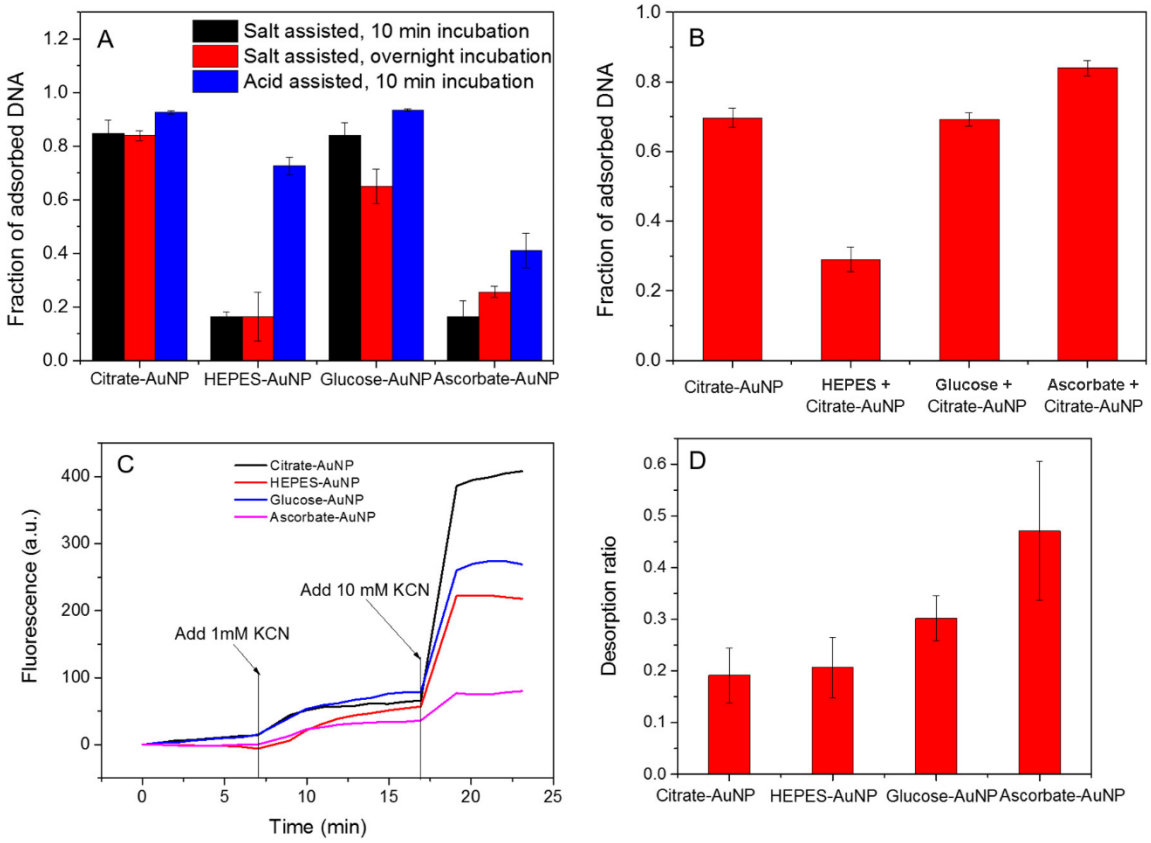

Figure 3. (A) The fraction of DNA adsorption by the four types of AuNPs assisted by salt or acid after 10 min or overnight incubation. (B) The fraction of DNA adsorption to the citrate-AuNPs in the presence of various reducing agents using the salt-assisted method after 10 min incubation. (C)

The kinetic traces of DNA desorption from the four kinds of AuNPs by adding different concentrations of KCN. (D) The fraction of DNA desorbed by 1 mM KCN from the AuNPs calculated by the fluorescence ratio between the fluorescence increase after adding 1 mM KCN and after adding 10 mM KCN.

Affinity of DNA adsorption studied by desorption

Since using acid can promote DNA adsorption to all the four types of the AuNPs, we then used this method to load DNA on AuNPs to study the stability of DNA adsorption. We adsorbed the FAM-DNA to the AuNPs using a 25:1 ratio and then added a low concentration (1 mM) of KCN to desorb the DNA (Figure 3C). With only 1 mM KCN, the AuNPs were not dissolved. Finally, a high concentration of KCN (10 mM) was added to fully dissolve the AuNPs and release all the remaining DNA. This allowed us to quantify the fraction of DNA desorbed by 1 mM KCN. Based on the fraction of DNA desorbed, the citrate-AuNPs and HEPES-AuNPs had stronger DNA adsorption affinities than the glucose-AuNPs and ascorbate-AuNPs (Figure 3D). The citrate and HEPES AuNPs allowed for more stable DNA adsorption, which might be explained by that HEPES and citrate adsorbed on AuNPs more strongly.[19] To compete with them, DNA needs to be adsorbed in a more stable conformation. Glucose and ascorbate can be more easily displaced by DNA under the acidic adsorption condition, and the adsorbed DNA was in turn more easily desorbed.

Label-free detection of DNA

We then compared the AuNPs for biosensing applications. A typical label-free DNA sensing scheme is shown in Figure 4A, where a single-stranded probe DNA can protect AuNPs from salt-induced aggregation. In the presence of a target DNA, a duplex is formed, resulting in a slow rate of adsorption to AuNPs which also leads to AuNPs aggregating into a cluster upon adding salt.[36-38] Therefore, for this sensing method to work, a quick adsorption of single-stranded DNA is required. Since the citrate-AuNPs and glucose-AuNPs both have better DNA adsorption ability and similar sizes, we focused on them in the sensing experiment.

We first mixed a 24-mer probe DNA with its target cDNA at different ratios, and the total DNA concentration was fixed at 1 μM. These DNA samples were respectively mixed with AuNPs

followed by a final addition of 100 mM NaCl solution.[39] Since the citrate-AuNPs showed a more obvious color change in the low concentration of dsDNA (Figure 4B), they had better sensitivity in the detection of the target DNA. As shown above, glucose had a lower affinity to AuNPs compared to citrate. DNA could more easily displace glucose from AuNPs and be adsorbed, and a small decrease in the single-stranded DNA concentration had only an insignificant effect on the stability of the glucose-AuNPs, leading to a lower sensitivity. Therefore, for the label-free DNA sensing, when the surface ligand is adsorbed too strongly or too weakly, the performance was not optimal. Citrate has the right affinity and the citrate-AuNPs were the best for such sensing applications.

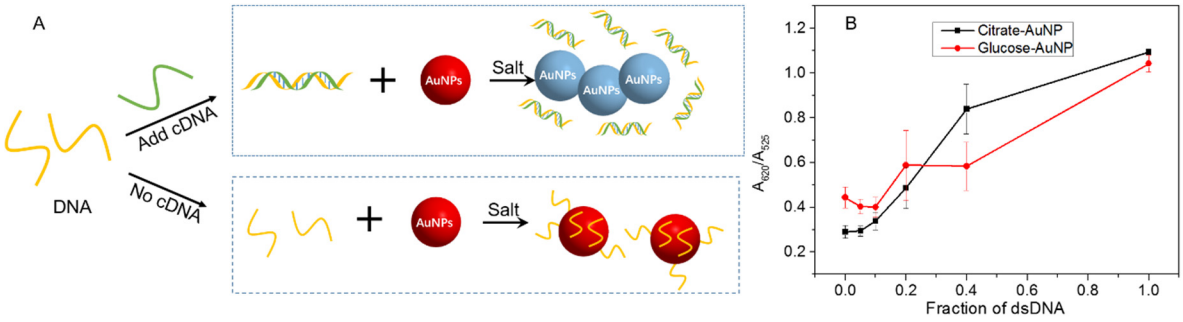

Figure 4. (A) A scheme showing the principle of label-free colorimetric sensing of DNA using AuNPs. (B) The absorbance ratio of the citrate-AuNPs and glucose-AuNPs as a function of the dsDNA fraction with a total DNA concentration of 1 μM.

Decreased colloidal stability and DNA adsorption upon aging of citrate-AuNPs

Since the affinity of citrate adsorption is important for sensor performance, and citrate may have time-dependent adsorption to AuNPs,[14] another goal of this work was to investigate the aging effect of AuNPs. Most previous studies focused on aging of DNA/AuNP conjugates,[40-42] while the study on the aging of AuNPs alone was less reported. A recent study showed that gold adatoms would gradually form and bind with the other terminal carboxylate of citrate upon aging of AuNPs.[14] Raman spectroscopy was previously used for characterizing citrate adsorption, but the effect of aging on sensing was not reported. Given the best performance of citrate-AuNPs and its popularity in sensing applications, we herein also studied its aging effect on DNA sensing. Since

the sensing performance is strongly affected by the colloidal stability of AuNPs and its ability to adsorb DNA, we first studied the aging effect on them.[39] In addition, aging was performed at ~22°C (room temperature) and in a 4°C fridge, which are storage conditions that AuNPs are typically kept.

We titrated NaCl to the AuNPs to measure their colloidal stability, which decreased gradually upon aging regardless of the storage temperature (Figure 5, Figure S3). The middle point where NaCl concentration induced aggregation was plotted against the aging time (Figure 5C). After 6 months, the shift in stability was about 5 to 10 mM NaCl. While this did not seem to be a large shift, it implies that the salt concentration needs to be individually optimized for aged AuNPs to achieve optimal sensing results.

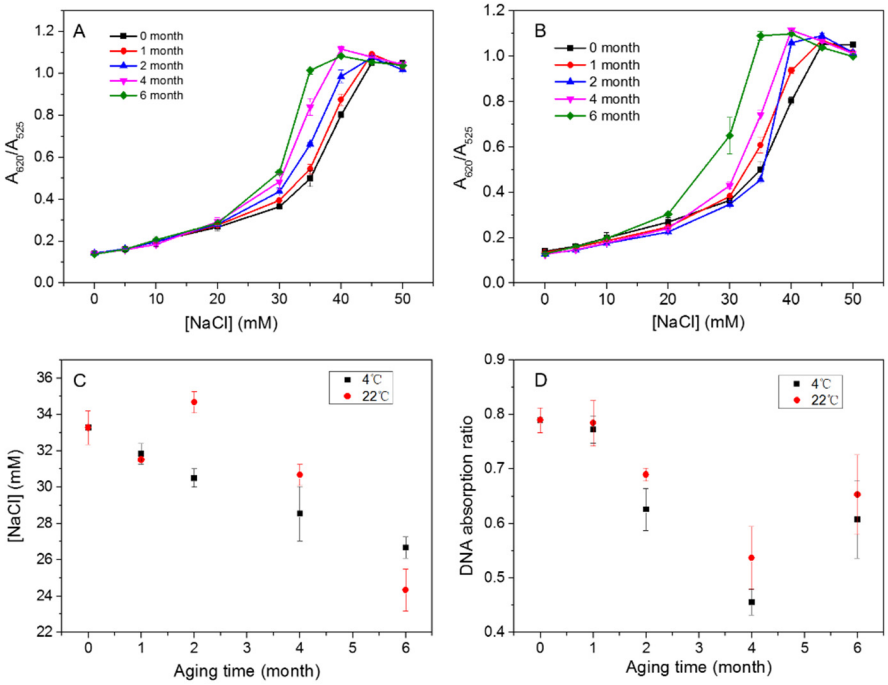

Figure 5. The effect of aging on the colloidal stability of citrate-AuNPs. The change of colloidal stability of citrate-AuNPs studied by adding NaCl for AuNPs stored at (A) 4°C and (B) room temperature, 22°C. (C) The middle point of the salt-dependent aggregation as a function of aging time for the AuNPs stored at 4°C and room temperature. (D) Fraction of DNA adsorption by the aged AuNPs at the two storage temperatures.

It was reported that the affinity for citrate became stronger upon aging of AuNPs.[14] Our observed trends of colloidal stability can be explained by it. Initially most citrate adsorbed with only one carboxyl group (Figure 6). When the other terminal carboxylate of citrate binds with the gold surface upon aging, the free space on AuNP surface is decreased. This also results in a decrease in the number of citrate ligand and the negative charge density on AuNPs. In addition, going from dangling citrate to chelating citrate may also make the negative charge closer to the AuNP surface, decreasing of the range of negative charge repulsion.

We then compared the DNA adsorption property of the aged AuNPs (Figure 5D). A decreasing trend was observed upon aging, although the drop was only around 20% over 6 months. Again, the influence of storage temperature was quite modest. With more strongly adsorbed citrate, the displacement of citrate by DNA was also more difficult, which can explain the decreased in DNA adsorption capacity (Figure 6).

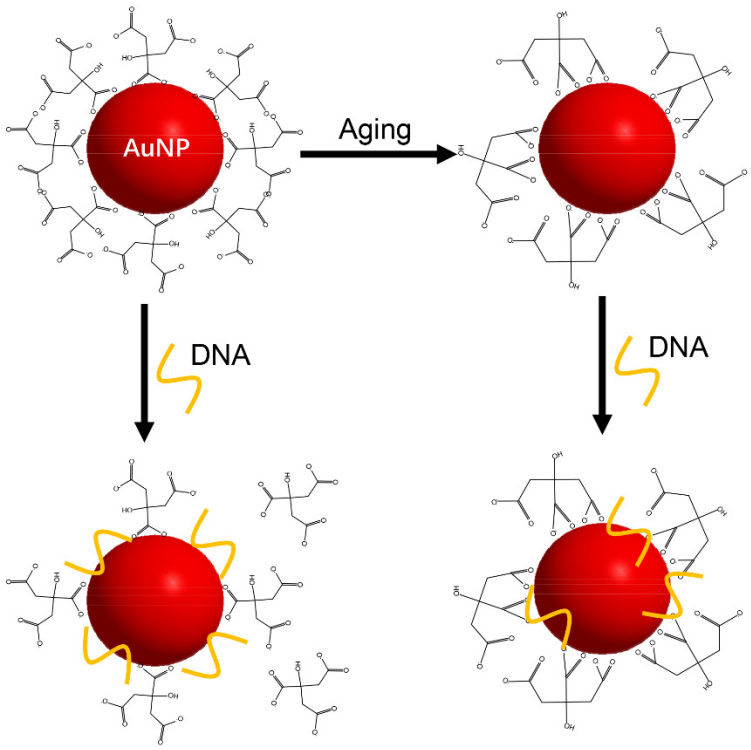

Figure 6. The schematic of the influence of aging for citrate-AuNP. Freshly prepared AuNPs have more citrate adsorption via terminal carboxylate, which upon aging converted to chelation of two carboxylate groups,[14] leading to decreased DNA adsorption capacity.

Decreased sensitivity for DNA detection upon aging of citrate-AuNPs

Since both the colloidal stability and DNA adsorption efficiency decreased upon aging, we speculated that the DNA sensing performance might also change. To test this hypothesis, we then did the label-free sensing experiment using the method described in Figure 4A. As shown in Figure 7A and 7B, for the aged AuNPs, the calibration curves gradually shifted to the right at both storage temperatures, indicating decreased sensitivity. To quantify the change in sensitivity, we plotted the slopes in the low dsDNA fraction region (0%, 5%, and 10% dsDNA) as a function of aging time (Figure 7C). The slopes (which is a measurement of sensitivity) decreased around 4-fold after 6 months, and the AuNPs stored at both temperatures showed a similar level of decrease (Figure S4).

Boiling cannot rescue the sensitivity of aged AuNPs

Since the decreased sensor performance was attributed to increased citrate adsorption stability, we wondered whether we could recover the sensitivity by heating. We refluxed the 7-month-aged AuNPs for 10 min. After cooling to room temperature, we then performed the sensing experiment (Figure S5). However, the sensitivity further decreased. This observation was consistent with the literature report that heating could not restore the way of citrate adsorption.[14] To refresh the AuNP surface, $HAuCl_4$ needs to be added in addition to heating. However, to add more $HAuCl_4$, the size of AuNPs might be changed so it is probably easier and more consistent to just synthesize fresh AuNPs.

It is well known that AuNPs can be stored for over 100 years and still retain a similar dispersed state and red color.[43] The stability and optical properties of AuNPs have made it attractive for developing biosensors. In the lab, it could well be that AuNPs prepared a long time ago are still being used, which could be a source of inconsistency in some label-free sensing experiments. For the best performance of label-free DNA detection, it is recommended that freshly prepared AuNPs are to be used. Although AuNPs still have the same color, their surface chemistry could be changed and such changes are cannot be easily quantified by UV-vis spectrometry (Raman and IR can be used for their characterization).[13, 14]

DNA adsorption on AuNPs is known to be caused from very strong base coordination interactions,[4] and adsorbed DNA cannot be easily displaced by even complementary DNA.[44] In

addition, citrate can also transition from weakly adsorbed to strongly adsorbed over time.[13, 14] Such strong adsorption affinities resulted in kinetic control of adsorption and slow kinetics in conformational changes of both DNA and citrate on AuNPs.

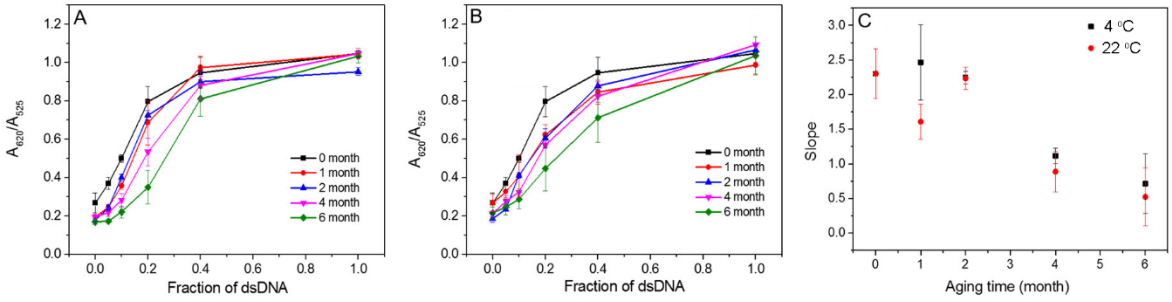

Figure 7. The effect of aging of citrate-AuNPs on the sensing performance for the AuNPs stored as (A) 4°C, and (B) room temperature of around 22°C. (C) The initial slopes at low dsDNA concentrations representing the sensitivity of the sensors using AuNPs with different aging times.

Conclusions

In this work, we first used four different common reducing reagents (citrate, glucose, ascorbate and HEPES) to synthesize AuNPs, and then did a series of studies on their colloidal stability, DNA adsorption capacity, and DNA adsorption affinity. The citrate-AuNPs and glucose-AuNPs had a better ability to adsorb DNA and showed higher affinity for the adsorbed DNA. After performing label-free DNA sensing experiments, we confirmed that citrate-AuNPs had the best sensing performance. Finally, we studied the influence of aging and storage temperature on the citrate-AuNPs. The citrate-AuNPs showed decreased colloidal stability and lower DNA adsorption efficiency upon aging. In addition, the aged citrate-AuNPs had decreased sensitivity for label-free colorimetric detection and the slope of the initial calibration curve dropped around 4-fold after 6 month storage. While we focused on the detection of DNA hybridization in this work, the conclusions should also be applicable for the detection of aptamer targets.[45-47] For aptamers, the adsorption of target molecules needs to be carefully studied to confirm feasibility of label-free detection.[38, 44, 48] This work articulated the effect of aging on the analytical performance of AuNPs and indicated that the sensing conditions need to be individually optimized as a function of storage time.

Supporting Information

Fluorescence intensity of different ratios of DNA and AuNPs, fluorescence intensity change of FAM-DNA by different adsorption methods with the four kinds of AuNPs, the UV-vis spectra of the effect of aging on the colloidal stability and sensing ability of citrate-AuNPs, the effect of heating on the sensing ability of citrate-AuNPs.

Acknowledgements

Funding for this work was from a Mitacs Accelerate grant and from the Natural Sciences and Engineering Research Council of Canada (NSERC).

References

(1) Saha, K.; Agasti, S. S.; Kim, C.; Li, X.; Rotello, V. M., Gold Nanoparticles in Chemical and Biological Sensing. *Chem. Rev.* **2012**, 112, 2739−2779.
(2) Chinen, A. B.; Guan, C. M.; Ferrer, J. R.; Barnaby, S. N.; Merkel, T. J.; Mirkin, C. A., Nanoparticle Probes for the Detection of Cancer Biomarkers, Cells, and Tissues by Fluorescence. *Chem. Rev.* **2015**, 115, 10530-10574.
(3) Li, L. L.; Xing, H.; Zhang, J. J.; Lu, Y., Functional DNA Molecules Enable Selective and Stimuli-Responsive Nanoparticles for Biomedical Applications. *Acc. Chem. Res.* **2019**, 52, 2415-2426.
(4) Liu, B.; Liu, J., Interface Driven Hybrid Materials Based on DNA-Functionalized Gold Nanoparticles. *Matter* **2019**, 1, 825-847.
(5) Aldewachi, H.; Chalati, T.; Woodroofe, M. N.; Bricklebank, N.; Sharrack, B.; Gardiner, P., Gold Nanoparticle-Based Colorimetric Biosensors. *Nanoscale* **2018**, 10, 18-33.
(6) Yao, G. B.; Li, J.; Li, Q.; Chen, X. L.; Liu, X. G.; Wang, F.; Qu, Z. B.; Ge, Z. L.; Narayanan, R. P.; Williams, D.; Pei, H.; Zuo, X. L.; Wang, L. H.; Yan, H.; Feringa, B.; Fan, C. H., Programming Nanoparticle Valence Bonds with Single-Stranded DNA Encoders. *Nature Mater.* **2020**, 19, 781–788.
(7) Tao, X.; Peng, Y.; Liu, J., Nanomaterial-Based Fluorescent Biosensors for Veterinary Drug Detection in Foods. *J. Food Drug Anal.* **2020**, 28, 575-594.
(8) Tseng, W. B.; Hsieh, M. M.; Chen, C. H.; Chiu, T. C.; Tseng, W. L., Functionalized Gold Nanoparticles for Sensing of Pesticides: A Review. *J. Food Drug Anal.* **2020**, 28, 521-538.
(9) Turkevich, J.; Stevenson, P. C.; Hillier, J., The Formation of Colloidal Gold. *J. Phys. Chem.* **1953**, 57, 670-673.
(10) Frens, G., Controlled Nucleation for the Regulation of the Particle Size in Monodisperse Gold Suspensions. *Nature* **1973**, 241, 20-22.
(11) Handley, D. A., Methods for Synthesis of Colloidal Gold. In *Coloidal Gold Principles, Methods, and Aplications*, 1 ed.; Hayat, M. A., Ed. Academic Press: San Diego, 1989; Vol. 1, pp 13-32.

(12) Al-Johani, H.; Abou-Hamad, E.; Jedidi, A.; Widdifield, C. M.; Viger-Gravel, J.; Sangaru, S. S.; Gajan, D.; Anjum, D. H.; Ould-Chikh, S.; Hedhili, M. N.; Gurinov, A.; Kelly, M. J.; El Eter, M.; Cavallo, L.; Emsley, L.; Basset, J.-M., The Structure and Binding Mode of Citrate in the Stabilization of Gold Nanoparticles. *Nat. Chem.* **2017**, 9, 890–895.
(13) Park, J.-W.; Shumaker-Parry, J. S., Structural Study of Citrate Layers on Gold Nanoparticles: Role of Intermolecular Interactions in Stabilizing Nanoparticles. *J. Am. Chem. Soc.* **2014**, 136, 1907-1921.
(14) Grys, D.-B.; de Nijs, B.; Salmon, A. R.; Huang, J.; Wang, W.; Chen, W.-H.; Scherman, O. A.; Baumberg, J. J., Citrate Coordination and Bridging of Gold Nanoparticles: The Role of Gold Adatoms in Aunp Ageing. *ACS Nano* **2020**, 14, 8689–8696.
(15) Park, J.-W.; Shumaker-Parry, J. S., Strong Resistance of Citrate Anions on Metal Nanoparticles to Desorption under Thiol Functionalization. *ACS Nano* **2015**, 9, 1665-1682.
(16) Deraedt, C.; Salmon, L.; Gatard, S.; Ciganda, R.; Hernandez, R.; Ruiz, J.; Astruc, D., Sodium Borohydride Stabilizes Very Active Gold Nanoparticle Catalysts. *Chem. Commun.* **2014**, 50, 14194-14196.
(17) Habib, A.; Tabata, M.; Wu, Y. G., Formation of Gold Nanoparticles by Good's Buffers. *Bull. Chem. Soc. Jpn.* **2005**, 78, 262-269.
(18) Xi, W.; Haes, A. J., Elucidation of HEPES Affinity to and Structure on Gold Nanostars. *J. Am. Chem. Soc.* **2019**, 141, 4034-4042.
(19) Huang, P.-J. J. J.; Yang, J.; Chong, K.; Ma, Q.; Li, M.; Zhang, F.; Moon, W. J.; Zhang, G.; Liu, J., Good's Buffers Have Various Affinities on Gold Nanoparticles Regulating Fluorescent and Colorimetric DNA Sensing. *Chem. Sci.* **2020**, 11, 6795-6804.
(20) Ebrahimi, S. B.; Samanta, D.; Mirkin, C. A., DNA-Based Nanostructures for Live-Cell Analysis. *J. Am. Chem. Soc.* **2020**, 142, 11343-11356.
(21) Wu, L.; Wang, Y.; Xu, X.; Liu, Y.; Lin, B.; Zhang, M.; Zhang, J.; Wan, S.; Yang, C.; Tan, W., Aptamer-Based Detection of Circulating Targets for Precision Medicine. *Chem. Rev.* **2021**, 121, 12035–12105.
(22) Laramy, C. R.; O'Brien, M. N.; Mirkin, C. A., Crystal Engineering with DNA. *Nat. Rev. Mater.* **2019**, 4, 201-224.
(23) Chen, G.; Gibson, K. J.; Liu, D.; Rees, H. C.; Lee, J. H.; Xia, W. W.; Lin, R. Q.; Xin, H. L. L.; Gang, O.; Weizmann, Y., Regioselective Surface Encoding of Nanoparticles for Programmable Self-Assembly. *Nat. Mater.* **2019**, 18, 169-174.
(24) Moon, W. J.; Liu, J., Interfacing Catalytic DNA with Nanomaterials. *Adv. Mater. Interfaces* **2020**, 7, 2001017.
(25) Ding, Y.; Jiang, Z.; Saha, K.; Kim, C. S.; Kim, S. T.; Landis, R. F.; Rotello, V. M., Gold Nanoparticles for Nucleic Acid Delivery. *Mol. Ther.* **2014**, 22, 1075-1083.
(26) Liu, B.; Wu, P.; Huang, Z.; Ma, L.; Liu, J., Bromide as a Robust Backfiller on Gold for Precise Control of DNA Conformation and High Stability of Spherical Nucleic Acids. *J. Am. Chem. Soc.* **2018**, 140, 4499–4502.
(27) Liu, J.; Lu, Y., Preparation of Aptamer-Linked Gold Nanoparticle Purple Aggregates for Colorimetric Sensing of Analytes. *Nat. Protoc.* **2006**, 1, 246-252.
(28) Turkevich, J.; Stevenson, P. C.; Hillier, J., A Study of the Nucleation and Growth Processes in the Synthesis of Colloidal Gold. *Discuss. Faraday Soc.* **1951**, 11, 55-75.
(29) Chen, R.; Wu, J.; Li, H.; Cheng, G.; Lu, Z.; Che, C.-M., Fabrication of Gold Nanoparticles with Different Morphologies in HEPES Buffer. *Rare Metals* **2010**, 29, 180-186.

(30) Suvarna, S.; Das, U.; Kc, S.; Mishra, S.; Sudarshan, M.; Saha, K. D.; Dey, S.; Chakraborty, A.; Narayana, Y., Synthesis of a Novel Glucose Capped Gold Nanoparticle as a Better Theranostic Candidate. *PloS one* **2017**, 12, e0178202.
(31) Malassis, L.; Dreyfus, R.; Murphy, R. J.; Hough, L. A.; Donnio, B.; Murray, C. B., One-Step Green Synthesis of Gold and Silver Nanoparticles with Ascorbic Acid and Their Versatile Surface Post-Functionalization. *RSC Adv.* **2016**, 6, 33092-33100.
(32) Zhang, X.; Servos, M. R.; Liu, J., Surface Science of DNA Adsorption onto Citrate-Capped Gold Nanoparticles. *Langmuir* **2012**, 28, 3896-3902.
(33) Zhang, X.; Liu, B.; Dave, N.; Servos, M. R.; Liu, J., Instantaneous Attachment of an Ultrahigh Density of Nonthiolated DNA to Gold Nanoparticles and Its Applications. *Langmuir* **2012**, 28, 17053-17060.
(34) Liu, B.; Liu, J., Methods for Preparing DNA-Functionalized Gold Nanoparticles, a Key Reagent of Bioanalytical Chemistry. *Anal. Meth.* **2017**, 9, 2633-2643.
(35) Borsook, H.; Davenport, H. W.; Jeffreys, C. E. P.; Warner, R. C., The Oxidation of Ascorbic Acid and Its Reduction in Vitro and in Vivo. *J. Biol. Chem.* **1937**, 117, 237-279.
(36) Li, H.; Rothberg, L., Colorimetric Detection of DNA Sequences Based on Electrostatic Interactions with Unmodified Gold Nanoparticles. *Proc. Natl. Acad. Sci. U.S.A* **2004**, 101, 14036-14039.
(37) Li, H.; Rothberg, L. J., Label-Free Colorimetric Detection of Specific Sequences in Genomic DNA Amplified by the Polymerase Chain Reaction. *J. Am. Chem. Soc.* **2004**, 126, 10958-10961.
(38) Zhang, F.; Liu, J., Label-Free Colorimetric Biosensors Based on Aptamers and Gold Nanoparticles: A Critical Review. *Anal. Sens.* **2021**, 1, 30-43.
(39) Ding, Y.; Liu, X.; Huang, P.-J. J.; Liu, J., Homogeneous Assays for Aptamer-Based Ethanolamine Sensing: No Indication of Target Binding. *Analyst* **2022**, 147, 1348-1356.
(40) Wang, L.; Wan, Y.; Xu, Q.; Lou, X., Long-Term Functional Stability of Functional Nucleic Acid–Gold Nanoparticle Conjugates with Different Secondary Structures. *Langmuir* **2019**, 35, 11791-11798.
(41) Bhatt, N.; Huang, P.-J. J.; Dave, N.; Liu, J., Dissociation and Degradation of Thiol-Modified DNA on Gold Nanoparticles in Aqueous and Organic Solvents. *Langmuir* **2011**, 27, 6132-6137.
(42) Li, F.; Zhang, H.; Dever, B.; Li, X.-F.; Le, X. C., Thermal Stability of DNA Functionalized Gold Nanoparticles. *Bioconjugate Chem.* **2013**, 24, 1790-1797.
(43) Thompson, D., Michael Faraday's Recognition of Ruby Gold: The Birth of Modern Nanotechnology. *Gold Bull.* **2007**, 40, 267-269.
(44) Zhang, F.; Wang, S.; Liu, J., Gold Nanoparticles Adsorb DNA and Aptamer Probes Too Strongly and a Comparison with Graphene Oxide for Biosensing. *Anal. Chem.* **2019**, 91, 14743-14750.
(45) Micura, R.; Höbartner, C., Fundamental Studies of Functional Nucleic Acids: Aptamers, Riboswitches, Ribozymes and DNAzymes. *Chem. Soc. Rev.* **2020**, 49, 7331-7353.
(46) Tao, X. Q.; Liao, Z. Y.; Zhang, Y. Q.; Fu, F.; Hao, M. Q.; Song, Y.; Song, E. Q., Aptamer-Quantum Dots and Teicoplanin-Gold Nanoparticles Constructed Fret Sensor for Sensitive Detection of Staphylococcus Aureus. *Chin. Chem. Lett.* **2021**, 32, 791-795.
(47) Tan, L. H.; Xing, H.; Lu, Y., DNA as a Powerful Tool for Morphology Control, Spatial Positioning, and Dynamic Assembly of Nanoparticles. *Acc. Chem. Res.* **2014**, 47, 1881-1890.

(48) Liu, X.; He, F.; Zhang, F.; Zhang, Z.; Huang, Z.; Liu, J., Dopamine and Melamine Binding to Gold Nanoparticles Dominates Their Aptamer-Based Label-Free Colorimetric Sensing. *Anal. Chem.* **2020**, 92, 9370–9378.

For TOC graphics only